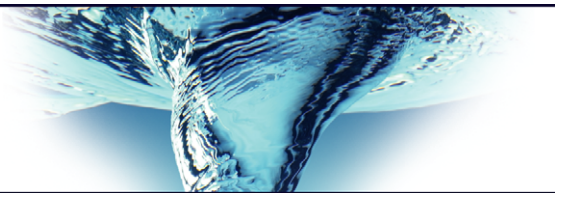
JFM RAPIDS
journals.cambridge.org/rapids



Axisymmetric gravity currents of power-law fluids over a rigid horizontal surface

Roiy Sayag† and M. Grae Worster

Department of Applied Mathematics and Theoretical Physics, University of Cambridge, Cambridge CB3 0WA, UK

(Received 12 August 2012; revised 20 September 2012; accepted 2 November 2012)

We analyse axisymmetric gravity currents of power-law fluids theoretically and experimentally. We use aqueous suspensions of Xanthan gum in laboratory experiments of constant-volume and constant-flux release to resolve the rheological parameters of the fluid, which we then compare with measurements made using a strain-controlled rheometer. We find that the constant-volume release of highly shear-thinning fluids involves an early-time evolution dominated by inertia, and non-convex free surfaces that make the application of similarity solutions of the late-time viscously dominated evolution inefficient at resolving material properties. In contrast, constant-flux release of the same fluids can be viscously dominated and consistent with the self-similar solution from early in the evolution, which makes it a more useful method for measuring rheological parameters.

Key words: complex fluids, geophysical and geological flows, non-Newtonian flows

1. Introduction

The propagation of axisymmetric, viscous gravity currents has been studied extensively for different configurations and fluid rheologies, and can be used, among other applications, to model geophysical flows on laboratory scales and to measure the rheological parameters of fluids.

Early studies of gravity currents of power-law fluids analysed the perfect-plastic limit (Nye 1952). The asymptotic evolution of Newtonian gravity currents was studied by Huppert (1982) using laboratory experiments and similarity solutions in which the position of the current front was found to be proportional to $t^{1/8}$ for a constant-volume release and to $t^{1/2}$ for a constant-flux release. The front evolution of a general power-law fluid having exponent n has been found to be proportional to $t^{1/(5n+3)}$ for a constant-volume release (Halfar 1983; Gratton, Minotti & Mahajan 1999), and to $t^{(2n+2)/(5n+3)}$ for a constant-flux release (Gratton *et al.* 1999; Balmforth *et al.* 2000). Similarity solutions have also been studied for a mass source that is proportional to the thickness and inversely proportional to time (Bueler *et al.* 2005).

† Email address for correspondence: rs620@cam.ac.uk

 © Cambridge University Press 2013
doi:10.1017/jfm.2012.545

https://doi.org/10.1017/jfm.2012.545 Published online by Cambridge University Press

Gravity currents are also being used to measure the rheological parameters of fluids. Devices such as the Bostwick and Adams consistometers provide quantitative measurements of rheological properties by finite-volume releases of fluid in a horizontal channel and axisymmetric geometries, respectively. The difficulty associated with the lateral friction at the sidewalls in channel geometry (Balmforth *et al.* 2007) is eliminated by the use of axisymmetric geometry (Piau & Debiane 2005). However, shear-thinning fluids in both geometries can undergo a slumping phase that is potentially dominated by inertia (Balmforth *et al.* 2007), followed by the viscous phase, which can be extremely slow for practical measurements. The presence of such a slumping phase may substantially reduce the efficacy of these systems as rheometers, yet so far this has not been assessed quantitatively.

In this study we present theoretical and experimental analysis of power-law fluids (zero yield stress) released with constant volume or constant flux in cylindrical geometry. We model an axisymmetric gravity current of low Reynolds number and derive similarity solutions for time-dependent volume release. We perform experiments, using highly shear-thinning suspensions, and demonstrate the dynamical differences that can arise between these two release mechanisms. In particular, we present completely new observations, with high temporal and spatial resolution, of the inertia-dominated regime in constant-volume experiments, and quantitatively evaluate the situations where inertia is important. For the constant-flux release we use our experimental results to predict the rheological parameters of the material used, and then compare our results to independent measurements made using standard rheometry techniques.

2. Theory

2.1. *Mathematical model*

Consider a fluid of viscosity μ and density ρ that propagates as a thin layer over a flat and rigid surface into an inviscid fluid of density $\rho - \Delta\rho$. Assuming the flow is axisymmetric, the radial force balance and the local and global mass balances within the limits of lubrication theory are, respectively,

$$\frac{\partial}{\partial z}\left(\mu\frac{\partial u}{\partial z}\right) = \rho g'\frac{\partial h}{\partial r}, \tag{2.1a}$$

$$\frac{\partial h}{\partial t} + \frac{1}{r}\frac{\partial}{\partial r}\left(r\int_0^h u\,\mathrm{d}z\right) = 0, \tag{2.1b}$$

$$2\pi\int_0^{r_N(t)} rh\,\mathrm{d}r = Qt^\alpha, \tag{2.1c}$$

where r, z, t are the radial, vertical and time coordinates respectively, u is the radial velocity of the viscous fluid and h its thickness, $g' = (\Delta\rho/\rho)g$, r_N is the position of the head of the current, and Qt^α is the total volume, where $\alpha = 0$ represents constant-volume release and $\alpha = 1$ represents constant-flux release (Huppert 1982). For a power-law fluid the effective dynamic viscosity is

$$\mu = \tilde{\mu}\left|\frac{1}{2}\frac{\partial u}{\partial z}\right|^{1/n-1}, \tag{2.2}$$

where $\tilde{\mu}$ is the consistency index and n is the flow-law exponent, which determines if the fluid is shear-thinning ($n > 1$) or shear-thickening ($n < 1$). The boundary conditions

https://doi.org/10.1017/jfm.2012.545 Published online by Cambridge University Press

at the fluid base and surface are

$$\mu\frac{\partial u}{\partial z}(z=h)=0, \quad u(z=0)=0, \tag{2.3a}$$

and at the head of the current $r=r_N$,

$$h=0, \quad q\equiv\int_0^h u\,\mathrm{d}z=h\dot{r}_N, \tag{2.3b}$$

where the dot denotes differentiation with respect to time, and the second condition can be derived by combining (2.1*b*) with the derivative of (2.1*c*) with respect to time, noting the source condition $\lim_{r\to 0}(2\pi rq)=\alpha Qt^{\alpha-1}$. Integrating (2.1*a*) and using (2.3*a*) gives

$$u(z)=-2^{1-n}\left(\frac{\rho g'}{\tilde{\mu}}\right)^n\left|\frac{\partial h}{\partial r}\right|^{n-1}\frac{\partial h}{\partial r}\frac{h^{n+1}}{n+1}\left[1-\left(1-\frac{z}{h}\right)^{n+1}\right]. \tag{2.4}$$

Integrating (2.4) over the fluid thickness and substituting the result into (2.1*b*) yields an ordinary differential equation for the current thickness:

$$\frac{\partial h}{\partial t}-\frac{2^{1-n}}{n+2}\left(\frac{\rho g'}{\tilde{\mu}}\right)^n\frac{1}{r}\frac{\partial}{\partial r}\left[r\left|\frac{\partial h}{\partial r}\right|^{n-1}\frac{\partial h}{\partial r}h^{n+2}\right]=0. \tag{2.5}$$

Equations (2.1*c*) and (2.5) admit a similarity solution

$$h(r,t)=\xi_N^{(n+1)/(2n+1)}Qb^{-2}t^{[\alpha(n+1)-2]/(5n+3)}\psi(\chi) \tag{2.6a}$$

in terms of the variable

$$\xi=rb^{-1}t^{-[\alpha(2n+1)+1]/(5n+3)}, \tag{2.6b}$$

where

$$b=\left[\frac{2^{1-n}}{n+2}\left(\frac{\rho g'}{\tilde{\mu}}\right)^n Q^{2n+1}\right]^{1/(5n+3)}, \quad \chi=\xi/\xi_N, \tag{2.7}$$

and $\xi_N=\xi(r=r_N(t))$. The dimensional radius of the current head is therefore

$$r_N=\xi_N bt^{[\alpha(2n+1)+1]/(5n+3)}. \tag{2.8}$$

These results are consistent with previous studies (Huppert 1982; Halfar 1983; Gratton *et al.* 1999; Balmforth *et al.* 2000). Substituting (2.6) into (2.5) and (2.1*c*), we find that $\psi(\chi)$ satisfies the equations

$$\left[\chi\psi'|\psi'|^{n-1}\psi^{n+2}\right]'+\frac{\alpha(2n+1)+1}{5n+3}\chi^2\psi'-\frac{\alpha(n+1)-2}{5n+3}\chi\psi=0, \tag{2.9a}$$

$$\xi_N=\left[2\pi\int_0^1\chi\psi(\chi)\,\mathrm{d}\chi\right]^{-(2n+1)/(5n+3)}, \tag{2.9b}$$

where the prime denotes $\mathrm{d}/\mathrm{d}\chi$, and the boundary conditions (2.3*b*) become

$$\psi=0, \quad \psi'|\psi'|^{n-1}\psi^{n+2}=0 \quad \text{at } \chi=1. \tag{2.9c}$$

Solutions to (2.9) for different α and n (figure 1) show that as n decreases the slope near the head of the current increases, and that the slope at both the axis of symmetry ($\chi=0$) and the head of the current increase with α. Below we discuss in more detail the solutions for $\alpha=0$ and for arbitrary $\alpha>0$.

https://doi.org/10.1017/jfm.2012.545 Published online by Cambridge University Press

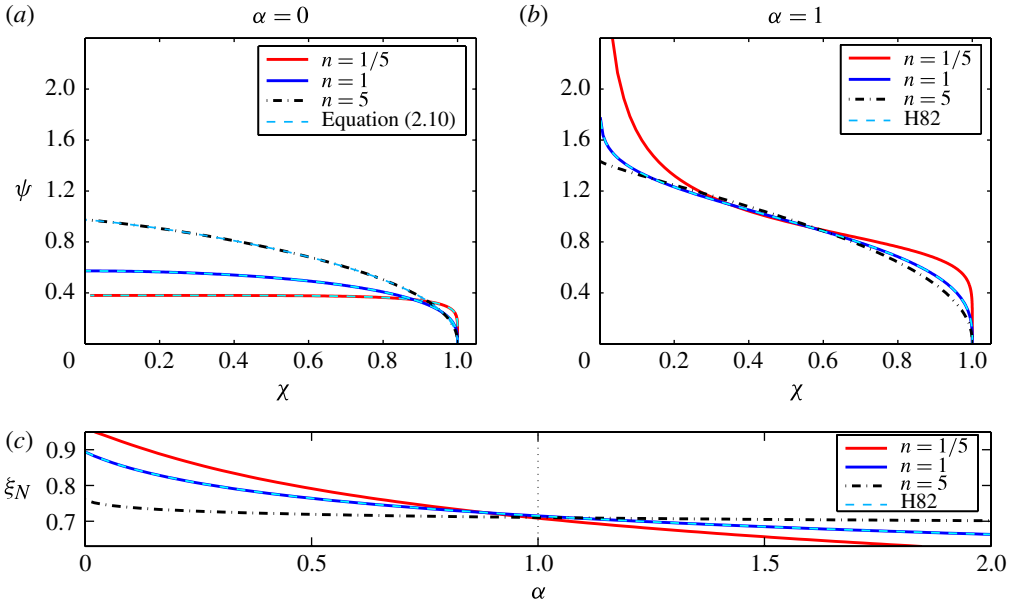


FIGURE 1. Numerical computation of the self-similar solutions of an axisymmetric gravity current of shear-thickening (solid red line, $n = 1/5$), Newtonian (solid black line, $n = 1$), and shear-thinning (dot-dashed line, $n = 5$) fluids, showing thickness profiles ψ for (a) constant-volume release compared with (2.10) (dashed line) and (b) for constant-flux release, and (c) the similarity variable at the current front ξ_N as a function of α. The solutions for $n = 1$ in (b, c) (dashed line) are consistent with Huppert (1982).

2.2. *Constant-volume release* ($\alpha = 0$)

In the case $\alpha = 0$ a closed-form solution exists for (2.9), given by

$$\psi = \left[\frac{2n+1}{n+1}\left(\frac{1}{5n+3}\right)^{1/n}\left(1-\chi^{(1+n)/n}\right)\right]^{n/(2n+1)}, \tag{2.10}$$

where

$$\xi_N = \left[\frac{2\pi n}{n+1}\left(\frac{2n+1}{n+1}\right)^{n/(2n+1)}\left(\frac{1}{5n+3}\right)^{1/(2n+1)} \times \frac{\Gamma\left(\dfrac{3n+1}{2n+1}\right)\Gamma\left(\dfrac{2n}{n+1}\right)}{\Gamma\left(\dfrac{3n+1}{2n+1}+\dfrac{2n}{n+1}\right)}\right]^{-(2n+1)/(5n+3)}, \tag{2.11}$$

as was previously found by Huppert (1982), and by Gratton *et al.* (1999) for the case $n = 1$. Note that the constant-volume solution (2.10), shown in figure 1(a) for $n = 1/5, 1, 5$, has zero slope at $\chi = 0$ for all values of n. This property is less apparent in the case $n > 1$ because the curvature near $\chi = 0$ behaves like $\psi''(\chi \sim 0) \sim -\chi^{(1-n)/n}$, which is singular for $n > 1$, leading to the apparent large

https://doi.org/10.1017/jfm.2012.545 Published online by Cambridge University Press

slope observed near $\chi = 0$.

2.3. *Solution for arbitrary* α

We estimate the solution for (2.9) using the leading-order asymptotic expansion at $\chi = 1$, which gives

$$\psi(\chi) = \left[\frac{\alpha(2n+1)+1}{5n+3}\left(\frac{2n+1}{n}\right)^n\right]^{1/(2n+1)}(1-\chi)^{n/(2n+1)}, \tag{2.12}$$

and is consistent with Huppert (1982) for $n = 1$. We then use (2.12) as an initial guess in the computation of numerical solutions to (2.9) for arbitrary α. A description of the numerical procedure we applied is given in the supplementary material available at http://dx.doi.org/10.1017/jfm.2012.545. We tested the numerical solver against the analytical solution for $\alpha = 0$ given in § 2.2 (figure 1*a*), and against solutions for $n = 1$ and arbitrary α (Huppert 1982) (figure 1*b,c*), and find very good agreement.

The numerical results indicate that for shear-thickening fluids ($n < 1$) the pressure gradient of the current near the origin becomes singular for $\alpha > 0$, whereas for shear-thinning fluids it is regular (figure 1). The scaled front position of the current ξ_N is monotonically decreasing with α for all n, and when $\alpha = 1$ it is nearly independent of n (figure 1*c*).

3. Experiments

To validate the theoretical prediction of the front position as a function of time (equation (2.8)), we performed a set of experiments of axisymmetric gravity currents at constant-volume ($\alpha = 0$) and constant-flux ($\alpha = 1$) release. In addition we performed an independent measurement of the viscosity using a strain-controlled rheometer. In all experiments we used an aqueous suspension of Xanthan gum of 1 % concentration by weight, which is known to be a shear-thinning material (e.g. Escudier *et al.* 2001).

3.1. *Constant-volume release*

The experimental setup for a constant volume release is shown in figure 2(*a,b*). The suspension (490 cm^3) was contained in a cylinder (64 mm inner diameter) with open ends that was initially in contact at its base with a flat aluminium surface. The cylinder was fixed to a pneumatic actuator, which when triggered moved at $\sim$70 cm s^{-1} in a vertical direction upward. The evolution of the discharged fluid was captured by a fast camera (2000 Hz) and the current thickness was measured along a radius by a laser sheet with a range finder (100 Hz). To enhance the laser reflection from the free surface, the Xanthan suspension was mixed with TiO_2 (0.25 % in weight), which modifies the rheology slightly but insignificantly, as indicated in later experiments performed with constant flux in § 3.2.

The propagation of the head of the current r_N (figure 3*a*), which was resolved from the thickness profiles (figure 3*b*), shows three dynamical regimes: (i) early-time evolution ($t < 0.35$ s) in which the front advances at 460 mm s^{-1} on average from a radius of 32 mm when confined in the cylinder to 180 mm; (ii) intermediate-time evolution ($0.35 < t < 0.5$ s) in which the front retreats back about 1 mm; and (iii) late-time evolution ($t > 0.5$ s) in which the front advances at 10^{-4} mm s^{-1} on average to a radius of $\sim$187 mm. On time scales longer than 10^4 s dehydration of the suspension becomes evident near the front as it retreats and leaves deposits on the aluminium surface.

https://doi.org/10.1017/jfm.2012.545 Published online by Cambridge University Press

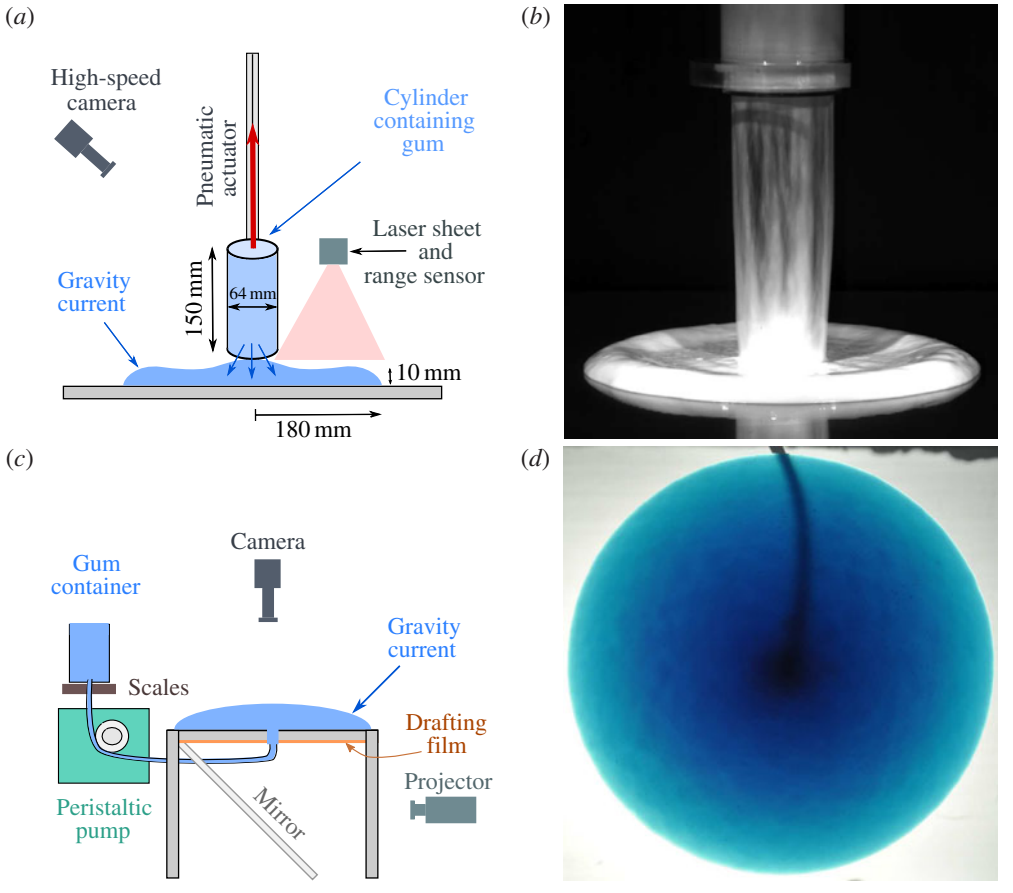


FIGURE 2. Schematic diagrams of the experimental apparatus used for (*a*) constant-volume release and (*c*) constant-flux release. Snapshot of (*b*) constant-volume experiment (oblique view), showing a thick ring of material at the head of the current (full evolution available in the accompanying video available at http://dx.doi.org/10.1017/jfm.2012.545), and (*d*) constant-flux experiment (plan view), showing an axisymmetric front.

The thickness evolution (figure 3*b*) reveals another level of complexity. During the early phase the propagating front is about three times thicker than the tail of the current. This bulged profile is roughly axisymmetric, as indicated in figure 2(*b*) and the associated video of the experiment (available at http://dx.doi.org/10.1017/jfm.2012.545), which is typical of high *Re* gravity currents. During the late-time evolution the free surface is non-convex, which leads to radial flow in both directions and is inconsistent with the similarity solution of § 2. These characteristics are inconsistent with the underlying assumptions of the similarity solution developed in § 2, and resolving those may require different analysis or incorporating additional physics, as we discuss in § 4.

3.2. *Constant-flux release*

The experimental setup for a constant-flux release (figure 2*c*) consisted of a peristaltic pump that drove the viscous fluid from a container and through a cylindrical nozzle

https://doi.org/10.1017/jfm.2012.545 Published online by Cambridge University Press

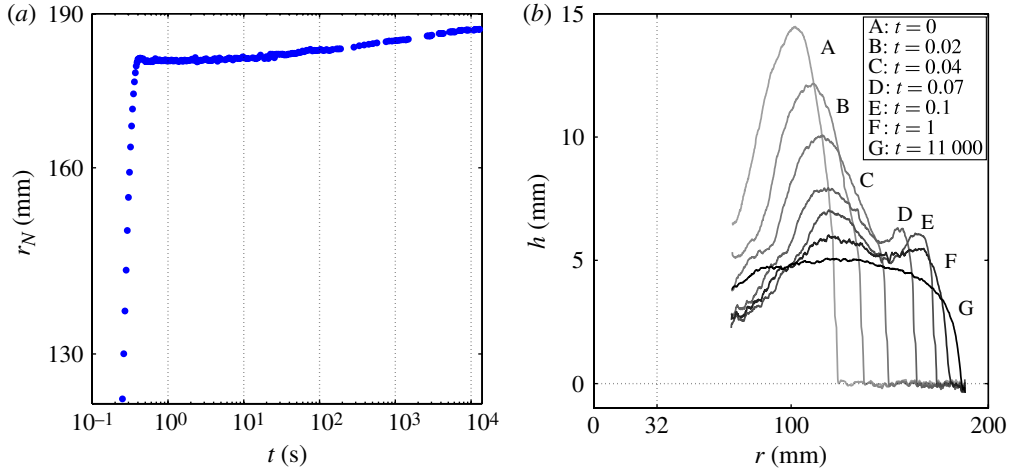


FIGURE 3. Experimental results of a constant-volume release of an aqueous suspension of Xanthan gum (1 % in weight). (*a*) The leading edge of the current r_N advances at a rate of 460 mm s^{-1} within the first 0.35 s and then slows down abruptly to an average rate of 10^{-4} mm s^{-1}. (*b*) Evolution of the current thickness along a radius (time shifted by 0.25 s). During the rapid phase the head of the current is substantially thicker than the tail, which implies that the flow is dominated by inertia. The dotted line at $r = 32$ mm marks the inner radius of the cylinder, which was lifted from the flat surface at $t = -0.25$ s. The $t = 0$ curve corresponds to the snapshot in figure 2(*b*).

onto a flat, transparent acrylic surface. The weight of the container as a function of time was recorded throughout the experiment and was used to compute the flux, which ranged between 3 and 10 g s^{-1} for the different experiments. Uniform light was projected from beneath the flat surface and a camera mounted above that surface took plan-view images (figure 2*d*) at constant time intervals (1–3 s) and of 5 pixels mm^{-1} resolution. By fitting a circle to each, we determined the evolution of the front radius r_N. We then computed a regression to the function $r_N = Ct^{\nu}$ (2.8), where $\nu = (2n + 2)/(5n + 3)$ and $C = \xi_N b$ were free parameters, including only the later part of the evolution that is consistent with the lubrication approximation. We estimate this by assuming that the total volume at each instant Qt is distributed in a disc shape with radius r_N and thickness $h = Qt/\pi r_N^2$, and then estimating the time when the lubrication approximation is satisfied by when the ratio $r_N/h = \pi r_n^3/Qt$ is larger than 10 (figure 4*a*). We find that $n \simeq 5.9 \pm 0.2$ and that $\tilde{\mu} = 11.4 \pm 0.25$ Pa s$^{1/n}$, where the uncertainties are the standard deviations (figure 4*b*). The suspension with TiO_2 that was used in the constant-volume experiments has $n \simeq 5.0 \pm 0.3$ and similar $\tilde{\mu}$.

3.3. *Strain-controlled rheometer*

As an additional and independent evaluation of the material parameters, we performed a series of shear-viscosity measurements using a strain-controlled rheometer (ARES). The measurements were performed using parallel plates of radius $R = 50$ mm and several gap sizes d, where the bottom plate was heated by a water jacket to keep the temperature constant (20 °C) and both plates were covered by a humidity cover to reduce evaporation. By specifying the rotation rate ω, the dynamical viscosity was measured for a range of shear rates $\dot{\gamma} \equiv (1/2)\partial u/\partial z = (1/2)R\omega/d$ varying between

https://doi.org/10.1017/jfm.2012.545 Published online by Cambridge University Press

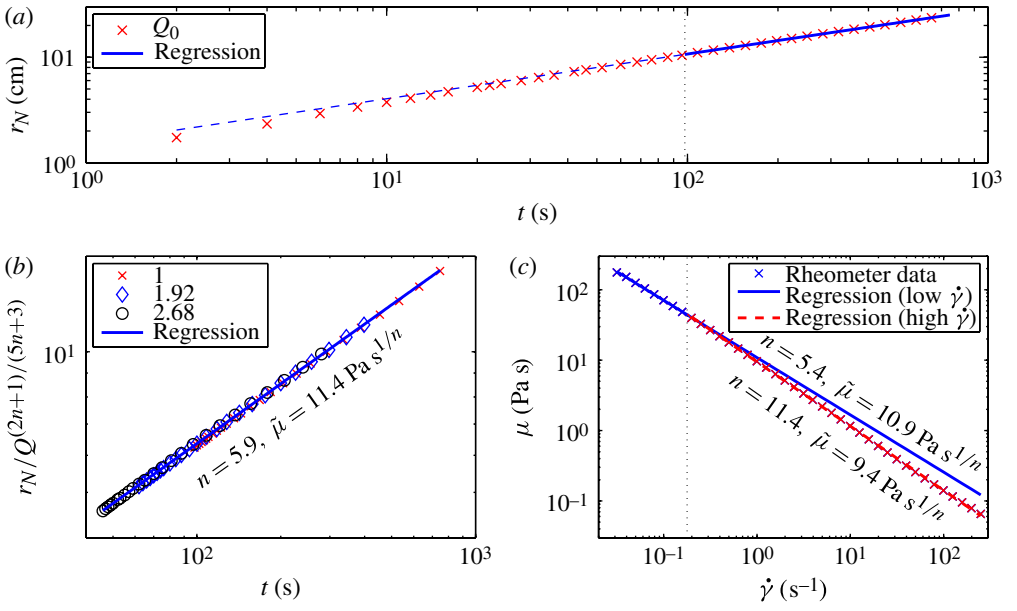


FIGURE 4. (*a*) The position of the leading edge r_N of a constant-flux ($Q_0 = 3$ g s^{-1}) gravity current as a function of time (×), and a regression to (2.8) with $\alpha = 1$ (solid line) using only the data with $r_N/h > 10$, which is on the right-hand side of the dotted line. (*b*) The normalized position r_N as a function of time for a range of inlet fluxes Q/Q_0 (×, ◇, ○) and the regression result (solid line). (*c*) The dynamic viscosity of the same suspension as a function of shear rate measured using a strain-controlled rheometer (×) is consistent with power-law rheology with exponent $n \simeq 5.4$ for low shear rates ($\dot{\gamma} \lesssim 0.1$ s^{-1}, solid line) and with $n \simeq 11.4$ for higher shear rates ($\dot{\gamma} \gtrsim 0.1$ s^{-1}, dashed line), where the consistency index is approximately 10 Pa s$^{1/n}$.

0.03 and 200 s^{-1} (figure 4*b*). We evaluate n and $\tilde{\mu}$ by regression to (2.2) in the range of shear rates associated with the constant-flux experiments in § 3.2. By order of magnitude the shear rate in those experiments is

$$\dot{\gamma} \sim \frac{U}{H} \sim \frac{R}{TH}, \tag{3.1}$$

where U is the radial-velocity scale, $R \sim 10$ cm is the radial length scale, $H \sim 1$ cm is the thickness scale, and $T \sim 100$–1000 s is the time scale. This implies that our constant-flux gravity-current experiments were in the range $\dot{\gamma} \sim 10^{-2}$–$10^{-1}$ s^{-1}. Therefore we compute the regression for $\dot{\gamma} \lesssim 0.1$ s^{-1} and find that $n \simeq 5.4$ and $\tilde{\mu} \simeq 10.9$. For $\dot{\gamma} > 0.1$ s^{-1} the parameters are $n \simeq 11.4$ and $\tilde{\mu} \simeq 9.4$ Pa s$^{1/n}$.

4. Discussion

Evaluation of the experiments done in §§ 3.1 and 3.2 using the viscous theory presented in § 2 requires us to validate that the underlying assumptions of the theory are satisfied during some interval in the experiment. In particular $Re \ll 1$ has to be satisfied. We can estimate Re for the viscous case based on the self-similar solutions

https://doi.org/10.1017/jfm.2012.545 Published online by Cambridge University Press

that were developed earlier. Specifically,

$$Re = \frac{\rho U H^2}{MR} = \frac{\rho}{\tilde{\mu}} \frac{U^{2-1/n} H^{1+1/n}}{R}, \tag{4.1}$$

where R, H are the radius and the thickness length scales, U is the velocity scale at the current surface and M is the viscosity scale given by (2.2). Using (2.4), (2.6*a*) and (2.8) we find

$$Re(t) = \frac{\rho}{\tilde{\mu}} \left[\frac{2^{1-n}}{n+1} \left(\frac{\rho g'}{\tilde{\mu}} \right)^n \right]^{2-1/n} Q_\alpha^{4n+1} b^{-2(5n+1)} t^{(2n\alpha - 2(5n+1))/(5n+3)}, \tag{4.2}$$

where we have assumed $\xi_N \sim \psi(\chi) \sim 1$. In particular, for $\alpha = 0, 1$ we have

$$Re(t, \alpha = 0) \sim \left(\tilde{\mu}^{-4n} Q_0^{3n+1} t^{-(10n+2)} \right)^{1/(5n+3)}, \tag{4.3a}$$

$$Re(t, \alpha = 1) \sim \left(\tilde{\mu}^{-4n} Q_1^{3n+1} t^{-(8n+2)} \right)^{1/(5n+3)}, \tag{4.3b}$$

where Q_0 represents volume and Q_1 represents volume flux. These expressions show that Re declines much faster in the constant-volume case than in the constant-flux case. The asymptotic behaviour for highly shear-thinning material ($n \gg 1$) is $Re \sim Q_0^{3/5} t^{-2}$ for $\alpha = 0$ and $Re \sim Q_1^{3/5} t^{-1.6}$ for $\alpha = 1$, while for highly shear-thickening fluid ($n \ll 1$) $Re \sim Q_\alpha^{1/3} t^{-2/3}$ independently of α.

Estimating Re for the constant-volume experiments performed in § 3.1 using $n = 5$ and $Q_0 \simeq 500$ cm^3, we find that $Re = 1$ near $t = 3$ s when all the volume has already been discharged, which implies that the early-time (slumping) phase is governed by inertia. This suggests that the late-time evolution of the constant-volume experiment may be consistent with the self-similar solutions in § 2. However, due to the inertia-dominated evolution at early times, the free surface of the gravity current is non-convex by the time $Re \ll 1$ (figure 3*b*), implying that the similarity solutions may only become useful at much later times, assuming no dehydration takes place.

In contrast, the constant-flux experiment with $n = 5$ and $Q_1 \simeq 10$ cm^3 s^{-1} becomes viscously dominated ($Re \lesssim 1$) at time $t \sim 1$ s, when the volume discharged (about 10 cm^3) is a small fraction of the total volume used compared with the finite-volume experiment. This implies that the similarity solutions in § 2 should predict the evolution of the constant-flux experiment from very early times, and can be used to predict the material properties, as was done in § 3.2.

The difference between the results of our constant-flux experiments and the rheometer measurements may be partly accounted for by experimental error, yet it is conceivable that a major part of the error is due to a non-power-law rheology, in particular at low strain rates. One potential non-power-law effect is the presence of a yield stress. To evaluate how significant a yield-stress effect may be we estimate the Bingham number,

$$B = \frac{\tau_0}{\mu U/H} = \frac{\tau_0 R}{\rho g' H^2}, \tag{4.4}$$

which is the ratio of the yield stress τ_0 to the shear stress $\sigma_{rz} = \mu \partial u/\partial z$, where the latter is evaluated using (2.1*a*). The yield stress for 1 % aqueous suspension of Xanthan is estimated as $\tau_0 \sim 10$ dyn cm^{-2} through a nonlinear regression to the Herschel–Bulkley model (Song, Kim & Chang 2006). Given that the density of the suspension is the same as that of water, then $g' \sim g$ and therefore $B \simeq 0.1$, which implies that the yield stress, if present, is insignificant in our gravity-current

https://doi.org/10.1017/jfm.2012.545 Published online by Cambridge University Press

experiments. This argument is also supported by numerical computations that power-law behaviour is hardly distinguishable from the yield-stress effect for a constant-flux source, and that the discrepancy between these two models diminishes with the increase of the exponent n (Balmforth *et al.* 2000).

The rheometer measurements may imply a yield-stress effect. However, this could be an artifact of the limited shear rates we measured, and may also appear due to insufficient sensitivity of strain-controlled rheometers at low shear rates (Balmforth *et al.* 2000). More sensitive measurements in the low-shear-rate regime performed with stress-controlled rheometers indicate that Xanthan suspensions of properties similar to those used here do become highly viscous, yet Newtonian at sufficiently low shear rates (Choppe *et al.* 2010). This implies that Xanthan rheology over a wide range of shear rates may be more consistent with Cross or Carreau–Yasuda models (Escudier *et al.* 2001), which suggests that a power-law approximation would be consistent only with a finite and narrow range of shear rates. This argument can explain why our gravity-current experiments, which were done in a narrow shear-rate range, are consistent with a power-law rheology (figure 4*a*), whereas the viscosity measured with the rheometer over a wider range of shear rates is better matched with a piecewise power-law relation with a declining exponent at smaller shear rates (figure 4*b*).

5. Conclusions

We analysed axisymmetric gravity currents of power-law fluids on a flat plane released in constant volume and constant flux, and compared theoretical predictions with laboratory experiments and rheometry measurements.

Our theoretical analysis focused on viscously dominated, self-similar solutions and is consistent with previous studies (Huppert 1982; Gratton *et al.* 1999; Balmforth *et al.* 2000). Laboratory experiments of constant-volume release of shear-thinning fluids demonstrated inertia-dominated evolution at early times with a non-convex free surface, and viscously dominated evolution at late times. Consequently, predicting the evolution of such flows using self-similar solutions of viscously dominated theory may be possible only at very late times. In addition, due to front propagation that is proportional to $t^{1/(5n+3)}$, measurements of such flows using highly shear-thinning fluids (large n) may take a long time (e.g. $r_N \propto t^{1/28}$ for $n = 5$) compared with constant-flux release, require more sensitive instruments, and can involve the risk of changes in material properties owing to external forcing such as dehydration. In contrast, a constant-flux release is viscously dominated from very early times, with fronts that propagate in proportion to $t^{(2n+2)/(5n+3)}$ (i.e. $r_N \propto t^{3/7}$ for $n = 5$), and can therefore be more useful for obtaining accurate measurements of a material rheology. Using this method to measure the rheological parameters of aqueous suspensions of Xanthan gum led to consistent results with rheometric measurements.

Measuring rheological properties of power-law fluids using a conventional rheometer requires numerous experiments of different shear rates. The viscous gravity current, following a power law in time, conveniently explores a range of shear rates in a single experiment. The particular geometry and fluid release mechanism of the setup that we propose is free of sidewalls and inertial effects, which are inherent to some industrial rheometers. This paper provides a protocol for a convenient method to determine the rheological properties of power-law fluids with sufficient accuracy to study various fluid-mechanical systems.

https://doi.org/10.1017/jfm.2012.545 Published online by Cambridge University Press

Acknowledgements

We thank M. R. Mackley for letting us use his laboratory rheometer and to S. Butler for assisting with the rheometer operation. We are also grateful to S. Dalziel, N. Vriend and the GK Batchelor Laboratory. RS is supported by a NERC fellowship.

Supplementary movie

Supplementary movie is available at http://dx.doi.org/10.1017/jfm.2012.545.

References

BALMFORTH, N. J., BURBIDGE, A. S., CRASTER, R. V., SALZIG, J. & SHEN, A. 2000 Visco-plastic models of isothermal lava domes. *J. Fluid Mech.* **403**, 37–65.

BALMFORTH, N. J., CRASTER, R. V., PERONA, P., RUST, A. C. & SASSI, R. 2007 Viscoplastic dam breaks and the Bostwick consistometer. *J. Non-Newtonian Fluid Mech.* **142** (1–3), 63–78.

BUELER, E., LINGLE, C. S., KALLEN-BROWN, J. A., COVEY, D. N. & BOWMAN, L. N. 2005 Exact solutions and verification of numerical models for isothermal ice sheets. *J. Glaciol.* **51** (173), 291–306.

CHOPPE, E., PUAUD, F., NICOLAI, T. & BENYAHIA, L. 2010 Rheology of Xanthan solutions as a function of temperature, concentration and ionic strength. *Carbohydrate Polym.* **82** (4), 1228–1235.

ESCUDIER, M. P., GOULDSON, I. W., PEREIRA, A. S., PINHO, F. T. & POOLE, R. J. 2001 On the reproducibility of the rheology of shear-thinning liquids. *J. Non-Newtonian Fluid Mech.* **97**, 99–124.

GRATTON, J., MINOTTI, F. & MAHAJAN, S. M. 1999 Theory of creeping gravity currents of a non-Newtonian liquid. *Phys. Rev.* E **60** (6), 6960–6967.

HALFAR, P. 1983 On the dynamics of the ice sheets. Part 2. *J. Geophys. Res.* **88** (NC10), 6043–6051.

HUPPERT, H. E. 1982 The propagation of two-dimensional and axisymmetric viscous gravity currents over a rigid horizontal surface. *J. Fluid Mech.* **121**, 43–58.

NYE, J. F. 1952 The mechanics of glacier flow. *J. Glaciol.* **2** (12), 82–93.

PIAU, J. M. & DEBIANE, K. 2005 Consistometers rheometry of power-law viscous fluids. *J. Non-Newtonian Fluid Mech.* **127**, 213–224.

SONG, K. W., KIM, Y. S. & CHANG, G. S. 2006 Rheology of concentrated Xanthan gum solutions: steady shear flow behaviour. *Fibers Polym.* **7** (2), 129–138.

https://doi.org/10.1017/jfm.2012.545 Published online by Cambridge University Press